Optimal Immunotherapy of Oncolytic Viruses and Adopted Cell Transfer in Cancer Treatment

G.V.R.K. VITHANAGE, SOPHIA R-J JANG
Department of Mathematics and Statistics
Texas Tech University
1108 Memorial Circle, Lubbock, TX 79409-1042
USA

Abstract: We investigate therapeutic effects of monotherapy of oncolytic viruses, of adopted cell transfer, as well as the two combined therapies over a short time treatment period by applying optimal control techniques. The goal is to minimize the number of susceptible tumor cells and the costs associated with the therapy over the treatment period. We verify that there exists an optimal control pair and derive the necessary conditions. The optimality system is solved numerically to provide optimal protocols under different scenarios with respect to initial tumor sizes and parameter values. Although the two types of therapy do not work synergistically when the viral killing rate by immune cells is large, a small anti-viral killing can improve therapy success of either monotherapy of oncolytic viruses or combined therapy of oncolytic viruses and adopted T cell transfer. This finding can be accomplished either by manipulating certain genes of viruses via genetic engineering or by chemical modification of viral coat proteins to avoid detection by the immune cells.

Key-Words: Tumor, Immune system, Oncolytic virus therapy, adoptive cell transfer, optimal control theory, Pontryagin's maximum principle

1 Introduction

Cancer immunotherapy is a promising strategy to treat cancer of various types. It consists of activating and harnessing the immune system to fight cancers [7, 31]. The therapy takes on several different approaches such as immune checkpoint inhibitors, adoptive cell transfer, monoclonal antibodies, cancer vaccines, and oncolytic virus therapy (OVT) [7, 31]. Adoptive cell transfer (ACT) is implemented through selecting and expanding patients' own tumor-specific T cells in vitro and then reinfusing back into patients to boost the patients' own immune ability to target cancer [16, 33]. Oncolytic viruses (OVs), on the other hand, are genetically engineered or naturally occurring viruses that selectively replicate in and kill cancer cells without harming the normal tissues [12, 31]. In recent years, an array of oncolytic viruses have demonstrated anti-tumor efficacy, including adenoviruses, herpes simplex viruses, measles viruses, vesicular stomatitis virus and New-castle disease virus [5, 14, 17, 31]. Compared with conventional treatment strategies, immune system activating agents produced by oncolytic viruses enable the infected tumor cells to be localized and concentrated, reducing possible side effects. In 2015, the USA Food and Drug Administration (FDA) approved *Talimogene Laherparepvec* (T-VEC), an herpes simplex virus, as the first oncolytic virus for the treatment of advanced melanoma [1, 10]. A wide variety of OVs

are currently going through studies in phase I/II clinical trials or in preclinical cancer models [1].

The interaction between tumor and tumor microenvironment is a very complicated process and this activity is changing rapidly. Mathematical modeling provides a valuable tool for understanding the complex interaction among the many components of the tumor microenvironment [8, 13]. Mathematical models can represent a natural phenomena by an equation system. This process can allow a more efficient and accurate analysis of the phenomenon. In addition to clinical and experimental research, mathematical and computational models can be very useful in studying various mechanisms involved in cancer development and can be used to illuminate the underlying dynamics of therapy systems, which can lead to more optimal treatment strategies.

The immune system interacts intimately with tumors over the entire process of disease development and progression. This complex cross talk between immunity and cancer cells can both inhibit and enhance tumor growth [7, 15, 36]. Recently, Vithanage et al. [37] proposed and investigated a mathematical model of tumor-immune system interactions with oncolytic viral therapy, wherein the immune cells can either be simulated to proliferate or be suppressed to increase their mortality. They concluded that reducing the viral killing rate by immune cells always increases the effectiveness of the viral therapy. The reduction of

anti-viral killing rate can be obtained by either manipulating certain genes of viruses via genetic engineering or by chemical modification of viral coat proteins to evade recognition by the immune cells [37]. However, their conclusion is based on the long term dynamical behavior of the tumor by analyzing the dynamical system of ordinary differential equations both analytically and numerically.

The goal of this work is to study short term effects of the therapy using optimal control theory. Several researchers have applied optimal control techniques to study OVT strategies [23, 28, 35]. For example, Kim et al. [23] investigated a tumor-immune system model with viral and immunotherapy in an optimal control setting. The immune cells in their model do not kill viruses and the infection rate is modeled by a simple mass action. Malinzi et al. [28] applied optimal control theory to study a model of tumor-immune system interactions with viral therapy and chemotherapy and they demonstrated numerically that viral therapy can enhance chemotherapy. Su et al. [35], on the other hand, studied a model with oncolytic viral therapy along with MEK inhibitor and compared optimal control strategy on the dosage of MEK inhibitor with the constant control strategy. Their simulations showed that the optimal control has better control effect than constant control.

In this investigation, the immune cells can kill viruses from the oncolytic therapy and the viral infection rate is modeled by a Michaelis-Menten kinetics. Specifically, the model of no optimal control is based on the work of Vithanage et al. [37] in which there are three boundary equilibria whereas the number of positive equilibria cannot be determined analytically. We will devise a best immunotherapy using optimal control theory techniques. In the following section, the mathematical model in [37] is revisited. An optimal control problem is introduced in Section 3 and the existence of an optimal control pair is verified. We apply the Pontryagin's maximum principle to derive the necessary conditions and the optimality system in the subsections. Section 4 presents numerical examples to illustrate monotherapy of OVT, of ACT, and a combination of OVT and ACT. The paper ends with a summary and conclusions in the final section.

2 A Mathematical Model

We first provide a brief description of the model studied in [37].

The tumor cells are classified into susceptible x and infected y. The compartment of free viral particles is denoted by v, and z is the collection of immune cells including both the innate and adaptive immune cells. The units of cell populations are numbers of cells and the unit of viral particles is given by pfu, the plaque-forming unit, with day as the time unit.

The susceptible tumor population x grows logistically with intrinsic growth rate r and carrying capacity $1/b$ for all tumor cells [26, 30, 34, 38, 40]. The mass action kinetics has been used by numerous researchers [22, 32, 34, 38] to describe viral infection of susceptible tumor cells. However, virus spread is likely to be slower, limited by spatial constraints [39]. Since viruses released from one infected cell cannot reach all susceptible tumor cells, the infection rate must be a saturating function of susceptible tumor cells [39]. As in [37], the infection process is modeled by a Michaelis-Menten term with a half saturation constant g and a maximum infection rate β. How the immune cells detect cancer cells and kill them is a complicated process [7]. It is assumed that the tumor killing by immune cells follows a mass action law [13, 25] and let k denote the rate by which susceptible tumor cells are killed by immune cells. The corresponding killing rate of infected tumor cells by immune cells is given by c. The infected tumor cells have an extra death rate a due to infection [30, 32, 34, 38].

Upon lyses, new progeny virions are released from infected tumor cells and the viral burst size per infected tumor cell is denoted by q [30, 32, 34, 38]. Immune cells recognize viruses as foreign pathogens and mount strong anti-viral responses which can eventually kill viruses from the OVT. We model this killing by the law of mass action with rate γ [3]. The natural death rates of viruses and immune cells are constant and are denoted by δ and d, respectively [34, 38]. As in [13, 25], it is assumed that there is a constant supply of immune cells from the lymph nodes into the tumor microenvironment at a rate s. When OVs infect and destroy cancer cells, specific antigens are released into the tumor microenvironment allowing immune cells to be activated [14, 29]. We use a Michaelis-Menten mechanism to model this activation from infected tumor cells [22, 30, 34] with p denoting the maximum rate and h the half saturation constant.

There are numerous mechanisms used by tumors to counter effect immune cells [7, 19]. Therefore, immune cells can either be stimulated to proliferate or be impaired to reduce their growth by susceptible cancer cells. A combination of stimulation and suppression on growth between cancer and immune cells may act simultaneously and may be modeled by the simple mass action at a rate m [13, 37]. The net growth increases or decreases due to presence of cancer cells can either be positive ($m > 0$), negative ($m < 0$) or null ($m = 0$). Negative m indicating tumor cells exert significant effect on the immune system leading to immunosuppression.

Based on the above descriptions, the model takes

the following form

$$x' = rx\left(1 - b(x+y)\right) - \frac{\beta xv}{g+x} - kxz$$

$$y' = \frac{\beta xv}{g+x} - ay - cyz$$

$$v' = qay - \delta v - \gamma vz \tag{1}$$

$$z' = s - dz + mxz + \frac{pyz}{h+y}$$

with the initial condition $x(0) > 0$, $y(0) \geq 0$, $x(0) + y(0) < 1/b$, $v(0) \geq 0$, $z(0) \geq 0$. All of the parameters r, b, β, k, a, c, q, δ, γ, s, d, p, h are positive except m which can be any real number. The negative m indicating the net effect of tumor on immune cells decreases their growth.

The authors in [37] provided several sufficient conditions in terms of model parameters for which the tumor can be eradicated for all sizes, that is, $\lim_{t\to\infty} x(t) = 0$ for all $0 < x(0) < 1/b$. In particular, if $m < 0$ and $k > \dfrac{r(bd-m)}{sb}$, then the tumor-free equilibrium $E_0 = (0,0,0,s/d)$ is globally asymptotically stable [37, Theorem 3.3]. However, it may take a very long time, longer than a patient's life time, to eliminate the tumor.

3 Optimal Control Problem

As elaborated above, the eradication results derived in [37] are with respect to the long term dynamics of the tumor, which may not be applicable in real life scenario. The aim of this section is to apply optimal control techniques to understand short term effects of immunotherapy relative to tumor regression. The goal is to minimize the number of susceptible tumor cells and the costs associated with immunotherapies over the finite treatment period $[0, T]$, where $T > 0$ is fixed.

Let $s_1 \geq 0$ and $s_2 \geq 0$ be the strengths of oncolytic viral therapy (OVT) and immunotherapy of adoptive cell transfer (ACT) respectively with $s_1 + s_2 > 0$. Denote $u_1(t)$ and $u_2(t)$ the controls for the OVT and ACT, respectively. In particular, the units of s_1 and s_2 are pfu day^{-1} and cell day^{-1} respectively, whereas u_1 and u_2 are dimensionless. The state equations take the following form

$$x' = rx\left(1 - b(x+y)\right) - \frac{\beta xv}{g+x} - kxz$$

$$y' = \frac{\beta xv}{g+x} - ay - cyz$$

$$v' = qay - \delta v - \gamma vz + s_1 u_1(t) \tag{2}$$

$$z' = s - dz + mxz + \frac{pyz}{h+y} + s_2 u_2(t)$$

and the initial condition are given by $x(0) > 0$, $y(0) \geq 0$, $x(0)+y(0) < 1/b$, $v(0) \geq 0$, $z(0) \geq 0$. Since the goal is to minimize susceptible tumor size as well as the costs of implementing immunotherapies over the treatment period $[0, T]$, the objective functional is written as

$$J(u_1, u_2) = \int_0^T \left(x(t) + \frac{c_1}{2}(u_1(t))^2 + \frac{c_2}{2}(u_2(t))^2\right)dt, \tag{3}$$

where (u_1, u_2) belonging to the class

$$U = \{(u_1, u_2) : u_i(t)\text{ is piecewise continuous with}$$
$$0 \leq u_i(t) \leq 1 \text{ on } [0, T], \ i = 1, 2\}. \tag{4}$$

The parameters $c_1 \geq 0$ and $c_2 \geq 0$ are the weighted constants used to balance the contributions between the two types of treatment. We assume $c_i > 0$ if $s_i > 0$. The optimal control problem consists of

$$\min_{(u_1, u_2)\in U} J(u_1, u_2) \tag{5}$$

subject to the state equations (2).

Once the optimal control problem is specified, we proceed to discuss the existence of optimal controls, their characterizations and the optimality system in the following subsections.

3.1 Existence of optimal control pair

Classical theory of optimal control [11] can be applied directly to study the problem formulated in (2)–(5). We first verify the existence of an optimal control pair.

Theorem 3.1. *There exists an optimal control pair for the problem (2)–(5).*

Proof. It is enough to show that the following conditions given in Corollary 4.1 of [11] are satisfied.

(a) The set of all initial conditions with a control pair $(u_1, u_2) \in U$ for which the state equations being satisfied is nonempty.

(b) U is closed and convex.

(c) The right hand side of each of the state equations is continuous, bounded above by the sum of the control and the state, and can be written as a linear function of $u_1(t)$, $u_2(t)$ with coefficients depending on time and the state.

(d) The integrand of $J(u_1, u_2)$ is convex in U and is bounded below by $-k_2 + k_1|(u_1, u_2)|^\eta$ with $k_1 > 0$ and $\eta > 1$.

Clearly for each fixed initial condition and control pair, (1) has a unique solution on $[0, T]$ and (a) is satisfied. Moreover, as $x'|_{x=0} = 0$, $y'|_{y=0} \geq 0$,

$v'|_{v=0} \geq 0$ and $z'|_{z=0} > 0$, solutions remain non-negative on $[0, T]$. It is obvious that (b) is true and (d) is satisfied with $\eta = 2$. To verify (c), notice $x(t) > 0$, $y(t) \geq 0$, $v(t) \geq 0$, $z(t) \geq 0$ and $0 < x(t) + y(t) < 1/b$ for all $t \in [0, T]$. Thus $x' \leq rx$, $y' \leq \beta v - ay$, $v' \leq qay - \delta v + s_1 u_1(t)$, and $z' \leq s - dz + pz + s_2 u_2(t)$ for $m < 0$ while $z' \leq s - dz + mz/b + pz + s_2 u_2(t)$ if $m \geq 0$, i.e.,

$$
\begin{pmatrix} x' \\ y' \\ v' \\ z' \end{pmatrix} \leq M \begin{pmatrix} x \\ y \\ v \\ z \end{pmatrix} + \begin{pmatrix} 0 \\ 0 \\ s_1 u_1(t) \\ s + s_2 u_2(t) \end{pmatrix},
$$

where

$$
M = \begin{pmatrix} r & 0 & 0 & 0 \\ 0 & -a & \beta & 0 \\ 0 & qa & -\delta & 0 \\ 0 & 0 & 0 & -d + m/b + p \end{pmatrix} \text{ if } m \geq 0
$$

and

$$
M = \begin{pmatrix} r & 0 & 0 & 0 \\ 0 & -a & \beta & 0 \\ 0 & qa & -\delta & 0 \\ 0 & 0 & 0 & -d + p \end{pmatrix} \text{ if } m < 0.
$$

Let $\mathbf{X} = (x, y, v, z)^{tr}$, the transpose of (x, y, v, z). Then

$$
||\frac{d\mathbf{X}}{dt}|| \leq ||M|| \cdot || \begin{pmatrix} x \\ y \\ v \\ z \end{pmatrix} || + || \begin{pmatrix} 0 \\ 0 \\ s_1 u_1 \\ s + s_2 u_2 \end{pmatrix} ||.
$$

Thus (c) is verified and there exists an optimal control pair for the control problem (2)–(5) by [11, pages 68-69]. □

3.2 The adjoint system and characterization of control pair

We apply the Pontryagin's maximum principle to derive necessary conditions [27]. Let $(\lambda_1, \lambda_2, \lambda_3, \lambda_4)$ denote the adjoint vector. The Hamiltonian of the op-timal control problem (2)–(5) is

$$
\begin{aligned}
&H(x, y, v, z, u_1, u_2, \lambda_1, \lambda_2, \lambda_3, \lambda_4) \\
&= x + \frac{c_1}{2}u_1^2 + \frac{c_2}{2}u_2^2 \\
&\quad + \lambda_1 \left(rx(1 - b(x + y)) - \frac{\beta xv}{x + g} - kxz \right) \\
&\quad + \lambda_2 \left(\frac{\beta xv}{x + g} - ay - cyz \right) \\
&\quad + \lambda_3 \left(qay - \delta v - \gamma vz + s_1 u_1 \right) \\
&\quad + \lambda_4 \left(s - dz + mxz + \frac{pyz}{h + y} + s_2 u_2 \right)
\end{aligned}
\tag{6}
$$

where the adjoint variables satisfy

$$
\lambda_1' = -\frac{\partial H}{\partial x}, \quad \lambda_2' = -\frac{\partial H}{\partial y},
$$

$$
\lambda_3' = -\frac{\partial H}{\partial v}, \quad \lambda_4' = -\frac{\partial H}{\partial z},
$$

with the transversality conditions

$$
\lambda_i(T) = 0 \text{ for } 1 \leq i \leq 4.
$$

Setting $\frac{\partial H}{\partial u_i} = 0$, $i = 1, 2$, we obtain $u_1 = \frac{-\lambda_3 s_1}{c_1}$ and $u_2 = \frac{-\lambda_4 s_2}{c_2}$. Since the controls u_1 and u_2 are bounded, $0 \leq u_1, u_2 \leq 1$, the characterization of the optimal control pair is therefore given by

$$
\begin{aligned}
u_1^*(t) &= \min \left\{ 1, \max\{0, \frac{-s_1 \lambda_3}{c_1}\} \right\} \\
u_2^*(t) &= \min \left\{ 1, \max\{0, \frac{-s_2 \lambda_4}{c_2}\} \right\}
\end{aligned}
\tag{7}
$$

provided $c_i > 0$, $i = 1, 2$. The above discussion is summarized as follows.

Proposition 3.1. *Given an optimal control pair* (u_1^*, u_2^*) *and solutions of the corresponding state equations (2), there exist adjoint variables* λ_i, $1 \leq$

$i \leq 4$, *satisfying*

$$
\begin{aligned}
\lambda_1' &= -1 - \frac{\beta g v}{(g+x)^2}\lambda_2 - mz\lambda_4 \\
&\quad - \left(r(1 - 2bx - by)\frac{\beta g v}{(g+x)^2} - kz \right)\lambda_1 \\[6pt]
\lambda_2' &= \lambda_1 rbs + (a + cz)\lambda_2 - qa\lambda_3 - \frac{phz}{(h+y)^2}\lambda_4 \\[6pt]
\lambda_3' &= \frac{\beta x}{g+x}\lambda_1 - \frac{\beta x}{g+x}\lambda_2 + (\delta + \gamma z)\lambda_3 \qquad (8)\\[6pt]
\lambda_4' &= kx\lambda_1 + cy\lambda_2 + \gamma v\lambda_3 \\
&\quad - \left(-d + mx + \frac{py}{h+y}\right)\lambda_4
\end{aligned}
$$

$$
\lambda_i(T) = 0, \ 1 \leq i \leq 4.
$$

Moreover, u_1^* and u_2^* are represented by (7).

The optimality system consisting of the state and adjoint equations is given as

$$
\begin{aligned}
x' &= rx\Big(1 - b(x + y)\Big) - \frac{\beta x v}{g + x} - kxz \\[6pt]
y' &= \frac{\beta x v}{g + x} - ay - cyz \\[6pt]
v' &= qay - \delta v - \gamma vz \\
&\quad + s_1 \min\left\{1, \max\{0, \frac{-s_1\lambda_3}{c_1}\}\right\} \\[6pt]
z' &= s - dz + mxz + \frac{pyz}{h + y} \\
&\quad + s_2 \min\left\{1, \max\{0, \frac{-s_2\lambda_4}{c_2}\}\right\} \\[6pt]
\lambda_1' &= -1 - \lambda_1\left(r(1 - 2bx - by) - \frac{\beta g v}{(g+x)^2} - kz\right) \\
&\quad - \lambda_2\frac{\beta g v}{(g+x)^2} - mz\lambda_4 \qquad (9)\\[6pt]
\lambda_2' &= rbx\lambda_1 + (a + cz)\lambda_2 - qa\lambda_3 - \frac{phz}{(h+y)^2}\lambda_4 \\[6pt]
\lambda_3' &= \lambda_1\frac{\beta x}{g+x} - \lambda_2\frac{\beta x}{g+x} + \lambda_3(\delta + \gamma z) \\[6pt]
\lambda_4' &= hx\lambda_1 + cy\lambda_2 + \gamma v\lambda_3 \\
&\quad - \lambda_4(-d + mx + \frac{py}{h+y})
\end{aligned}
$$

with boundary conditions $x(0) > 0$, $y(0) \geq 0$, $v(0) \geq 0$, $z(0) > 0$, $x(0) + y(0) < 1/b$, $\lambda_i(T) =$

0, $1 \leq i \leq 4$. The optimality system (9) yields a two-point boundary value problem. It can be verified as in [2, 20] that the solution of (9) is unique if $T > 0$ is small.

4 Numerical Investigations

We apply the numerical technique of backward-forward sweep method described in [27] combined with the fourth-order Runge-Kutta scheme to numerically solve the optimality system (9).

Before numerical explorations, a plausible range of parameter values and their sources are provided in Table 1 with the baseline values given in equation (10). There is a wide range of tumor growth rates in the literature. For example, $r = 0.18$ in [25], $r = 0.514$ in [6, 13], and $r \in (0.69, 0.97)$ are adopted in [9]. In the review paper [9], tumor growth rates of 0.23, 0.43 and 1.636 are simulated in the numerical examples to demonstrate model outcomes. Motivated by the work in [21], the tumor growth rate is estimated using the doubling time of about 48-60 hours of the BxPC-3 cell line [4] by assuming an initial exponential growth phase. These parameter values were also adopted in the numerical investigations in [37].

Parameter	Value	Reference
r	0.2773–0.3466 day^{-1}	[37]
b	1.02× 10^{-9} cell^{-1}	[6]
β	6×10^{-12}–0.862 cell pfu^{-1}day^{-1}	[9]
k	10^{-5}–10^{-3} cell^{-1}day^{-1}	[13]
a	1.333–2.6667 day^{-1}	[13]
c	0.0096–4.8 cell^{-1}day^{-1}	[13]
q	10–1350 pfu day^{-1}	[13]
δ	0.024–24 day^{-1}	[34]
γ	0.024–48 cell^{-1}day^{-1}	[34]
m	-1–1.5×10^{-9} cell^{-1}day^{-1}	[13]
p	2.4×10^{-4}–2.5008 day^{-1}	[34]
h	20–5×10^4 cell	[34]
s	5×10^3 cell day^{-1}	[13]
d	2 day^{-1}	[13]
g	40–10^5 cell	[30]
s_1	varied pfu day^{-1}	
s_2	varied cell day^{-1}	
u_1	0–1 dimensionless	[27]
u_2	0–1 dimensionless	[27]

Table 1: Parameters values and their sources

The baseline parameter values are given by

$$
\begin{aligned}
r &= 0.346, \ b = 1.02 \times 10^{-9}, \ a = 1.333, \ c = 1.8, \\
q &= 100, \ d = 2, \ \delta = 1.83, \ p = 2.4 \times 10^{-4}, \quad (10)\\
h &= 5 \times 10^4, \ g = 10^5, s = 5 \times 10^3,
\end{aligned}
$$

and we vary the parameter values of β, γ, m and k. Unless otherwise stated, $c_1 = 10$ and $c_2 = 10$ are used when the corresponding therapy is applied. The values of c_1 and c_2 are chosen arbitrary. However,

if we vary these values we obtain similar simulation results.

In [24], 5×10^6 human BxPC-3 cells of pancreatic ductal adenocarcinoma were injected into mice subcutaneously. When the tumor had grown to a diameter of 5–7 mm, two different oncolytic viruses at a MOL of 10^8 pfus were injected subcutaneously to different groups of mice. Therefore, the dosage s_1 of OVT is varied around 10^8 pfus. In [18], 10^5 to 2×10^6 number of T cells were infused to the experimental mouse. In our numerical examples, the values of s_1 and s_2 are hypothetical but are close to the values of above experiments.

We first consider the monotherapy of OVT, of ACT, and then the combined immunotherapy of OVT and ACT in the following subsections.
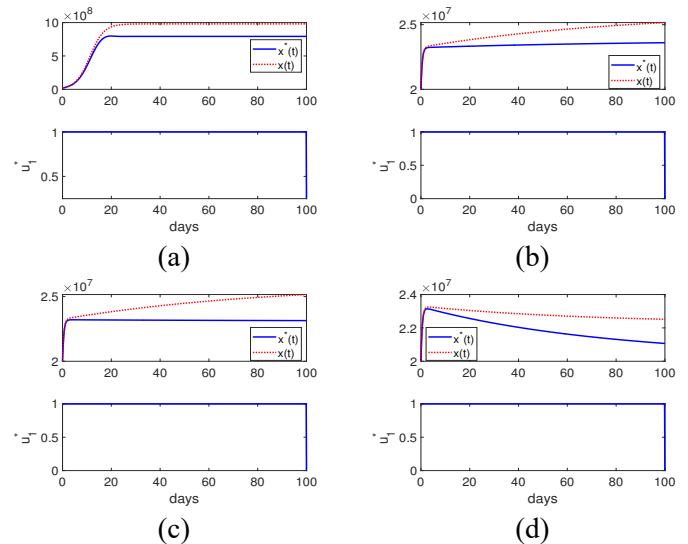

Figure 1: $s_1 = 10^8$ and $\beta = 0.6$ with $\gamma = 0.9$ in (a), (b) and (d), and $\gamma = 0.7$ in (c). (a) $m = -10^{-6}$, $k = 10^{-5}$. (b)–(c) $m = 10^{-9}$, $k = 1.33 \times 10^{-4}$. (d) $m = 1.5 \times 10^{-9}$, $k = 1.33 \times 10^{-4}$.

4.1 Monotherapy of oncolytic viruses

We explore the situation when only the OVT is applied by letting $c_2 = s_2 = 0$.

First, consider the strength s_1 of OVT as $s_1 = 10^8$ with a fixed treatment period of 100 days, i.e., $T = 100$. Unless otherwise stated, the initial condition is chosen as

$$(x(0), y(0), v(0), z(0)) = (2 \times 10^7, 0, 0, 300),$$

which is the larger tumor size given in the numerical examples of [37]. The simulation results are provided in Figures 1–4, where the susceptible tumor sizes of no therapy denoted by $x(t)$ and of optimal OVT represented by $x^*(t)$ are plotted in the top row. The bottom row plots the corresponding optimal controls $u_i^*(t)$. Figure 1 shows that the OVT has to be performed during the whole treatment period in order to control the tumor. Notice that the susceptible tumor is increasing in Figure 1(b) and 1(c) when there is no therapy, and it is either stabilized in Figure 1(b) or slowly decreases in Figure 1(c) during the whole treatment period. With the parameter values in Figure 1(d), the tumor size is decreasing slowly when no OVT is applied. However, the OVT has to be applied for the whole treatment period in order to reduce the susceptible tumor size more effectively.
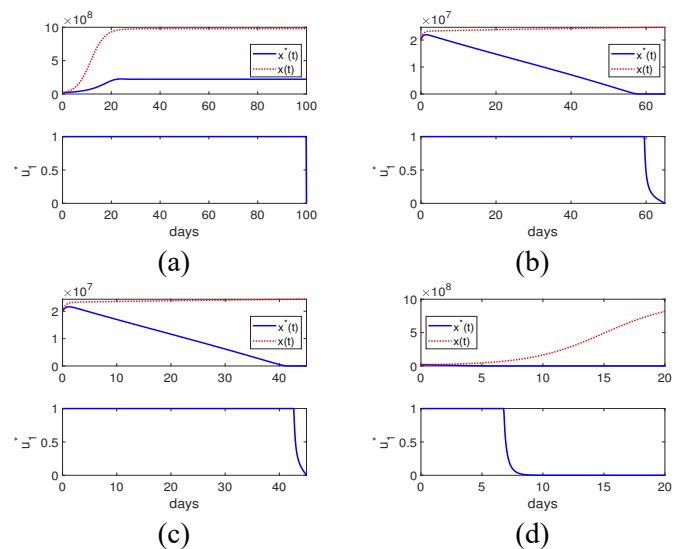

Figure 2: Parameters $s_1 = 10^8$ and $\gamma = 0.05$ are fixed. (a) $m = -10^{-6}$, $\beta = 0.6$, $k = 1.33 \times 10^{-4}$. (b) $m = 10^{-9}$, $\beta = 0.6$, $k = 1.33 \times 10^{-4}$ with $T = 65$. (c) $m = 10^{-9}$, $\beta = 0.8$, $k = 1.33 \times 10^{-4}$. (d) $m = -10^{-6}$, $\beta = 0.8$, $k = 10^{-3}$.

Next, $s_1 = 10^8$ with $\gamma = 0.05$ are simulated and the results are provided in Figure 2. The viral killing rate by immune cells is smaller than in Figure 1 and we can see that the OVT is more effective. Particularly, the treatment period can be shortened to 65 days in Figure 2(c) as the susceptible tumor cells are eradicated by day 60 using the OVT alone. Comparing

Figure 2(c) and (d), there is a change in tumor killing rate k but a huge difference between the two treatment outcomes even though the tumor microenvironment is more immunosuppressive in Figure 2(d).

In Figure 3 we choose the viral infection rate β as 0.8 and let $\gamma = 0.05$ with various values of m and k. When the tumor killing rate k is increased from 10^{-4} to 1.33×10^{-4}, the susceptible tumor is eradicated by day 45 shown in Figure 3(a) and (b). If tumor is more immunosuppressive but with a larger tumor killing rate $k = 10^{-3}$, the tumor can be eliminated by day 10 as illustrated in Figure 3(d). On the contrary, the tumor cannot be eradicated if the tumor killing rate is smaller with $k = 10^{-4}$ in Figure 3(c).

Figure 4: $s_1 = 10^6$, $\beta = 0.6$, $m = -10^{-6}$, and $(x(0), y(0), v(0), z(0)) = (10^7, 0, 0, 300)$. (a) $k = 10^{-5}$, $\gamma = 0.15$. (b) $k = 10^{-4}$, $\gamma = 0.15$. (c) $k = 10^{-5}$, $\gamma = 0.25$. (d) $k = 10^{-4}$, $\gamma = 0.25$. The susceptible tumor without treatment and with OVT are given by $x(t)$ and $x^*(t)$ respectively.
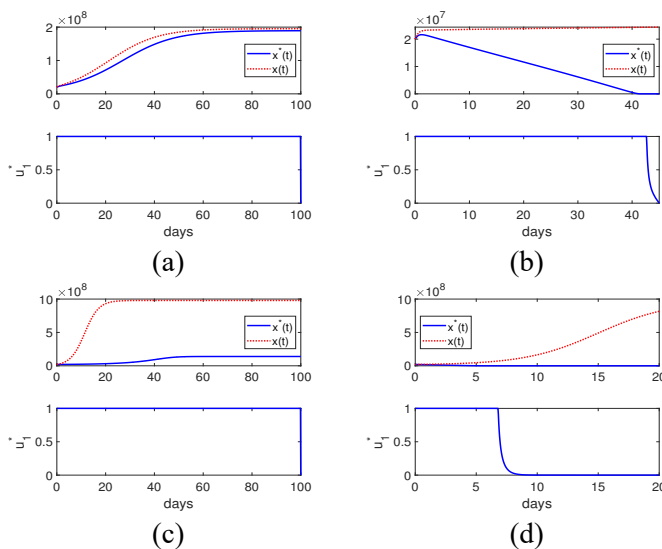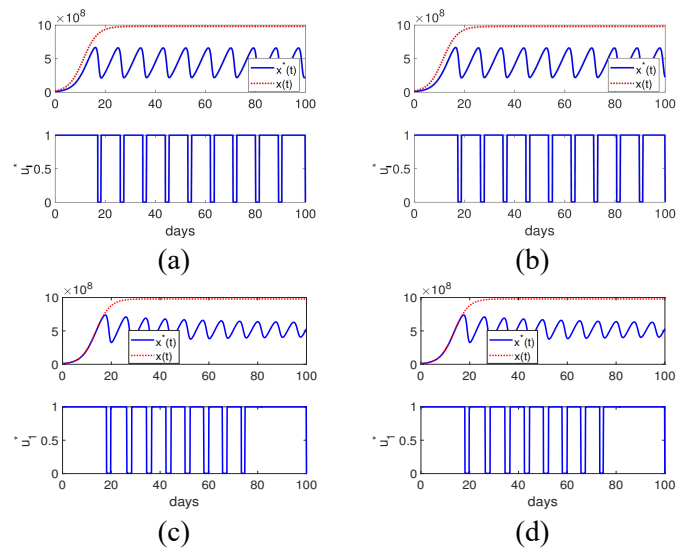

Figure 3: $s_1 = 10^8$, $\beta = 0.8$ and $\gamma = 0.05$. (a) $m = 10^{-9}$, $k = 10^{-4}$. (b) $m = 10^{-9}$, $k = 1.33 \times 10^{-4}$ with $T = 45$. Notice that $x^*(t)$ becomes extinct by $t = 45$. (c) $m = -10^{-6}$, $k = 10^{-4}$. (d) $m = -10^{-6}$, $k = 10^{-3}$, $T = 20$.

In the next figure, Figure 4, we let $\beta = 0.6$, $m = -10^{-6}$ but with a smaller initial tumor size $(10^7, 0, 0, 300)$. In this scenario, the susceptible tumor is oscillating over the treatment period with sizes smaller than the tumor with no treatment. In addition, the therapy needs not to be implemented for the whole treatment period. There are short periods of times when no therapy is required. We also simulated the cases that correspond to Figure 4 with $c_1 = 100$. Similar results are obtained and they are not presented.
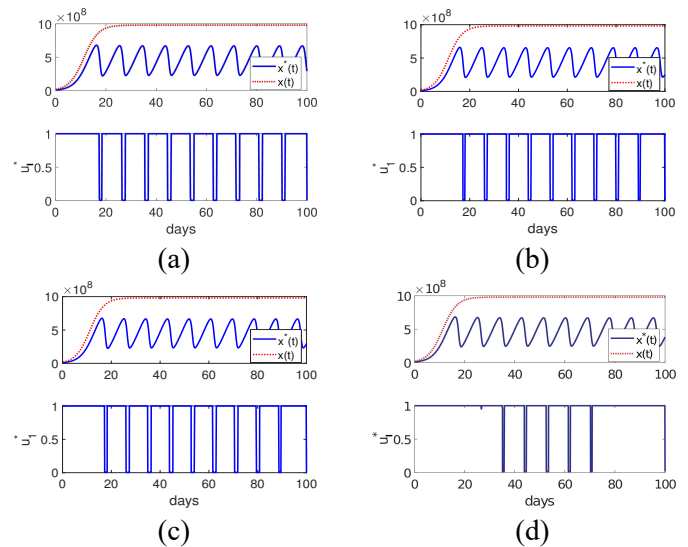

Figure 5: $s_1 = 10^6$, $m = -10^{-6}$, $k = 10^{-5}$, and $(x(0), y(0), v(0), z(0)) = (10^7, 0, 0, 300)$ are fixed. (a) $\beta = 0.58$, $\gamma = 0.15$. (b) $\beta = 0.61$, $\gamma = 0.15$. (c) $\beta = 0.6$, $\gamma = 0.16$. (d) $\beta = 0.6$, $\gamma = 0.17$. The susceptible tumor without treatment and with OVT are given by $x(t)$ and $x^*(t)$ respectively

Figure 5 presents simulation results with a smaller tumor size $x(0) = 10^7$ under different scenarios. The only difference between (a) and (b) is the viral infec-

tion rate, where β is 0.58 in (a) and 0.61 in (b), and their effect is small with respect to the timing of therapy as well as susceptible tumor size. In (c) and (d), the viral infection rate β is the same but with different viral killing rate γ. It is 0.16 in (c) and 0.17 in (d). With a slight larger viral killing rate, the viral therapy will need to apply for a longer period of time in order to control the tumor.

4.2 Monotherapy of adopted cell transfer

In this subsection, monotherapy of adopted immune cell transfer (ACT) is considered, i.e., $c_1 = s_1 = 0$. If there are no virus and infected tumor cells initially, $v(0) = 0 = y(0)$, then since only ACT is applied, it is sufficient to consider the xz-subsystem with ACT. In particular, parameter values of β and γ will not affect treatment outcome.
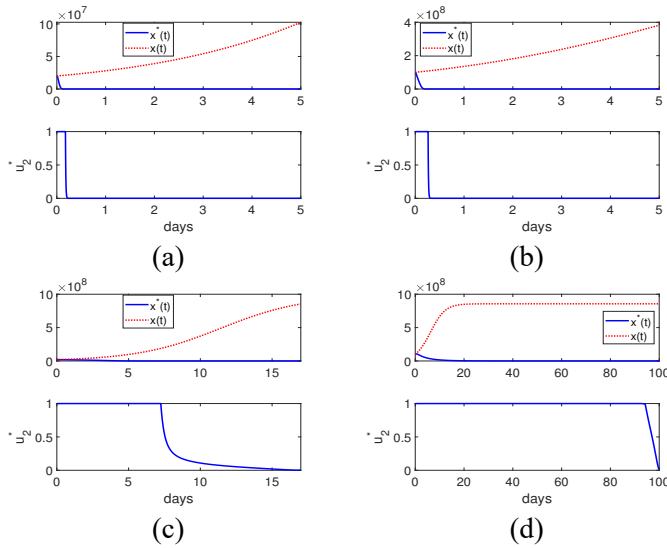

(a)

(b)

(c)

(d)

Figure 6: (a) $m = -10^{-6}$, $k = 10^{-5}$, $s_2 = 10^8$, and $(x(0), y(0), v(0), z(0)) = (2 \times 10^7, 0, 0, 300)$. (b) $m = -10^{-6}$, $k = 10^{-5}$, $s_2 = 10^8$, $(x(0), y(0), v(0), z(0)) = (10^8, 0, 0, 300)$. (c) $m = 10^{-9}$, $k = 10^{-5}$, $s_2 = 10^8$, $(x(0), y(0), v(0), z(0)) = (2 \times 10^7, 0, 0, 300)$. (d) $m = 10^{-9}$, $k = 10^{-5}$, $s_2 = 10^5$, $(x(0), y(0), v(0), z(0)) = (10^8, 0, 0, 300)$. The susceptible tumor without treatment and with OVT are given by $x(t)$ and $x^*(t)$ respectively

The parameter values $m = -10^{-6}$ and $k = 10^{-5}$ are fixed in Figure 6(a)-(b) and we vary s_2 and the initial susceptible tumor size. In this scenario, the critical immune cell size needed to eradicate susceptible tumor cells derived in [37] is 3.3991×10^7. From Figure 6(a), we see that with an ACT strength of $s_2 = 10^8$ the $x^*(t)$ can be eliminated within the first 5 days. We increase the initial tumor size $x(0)$ to 10^8 in Fig-

ure 6(b) and obtain a similar conclusion. In Figure 6(c)-(d), the tumor microenvironment is less suppressive with $m = 10^{-9}$. The result shows that a smaller tumor size can be eradicated by day 100 using only $s_2 = 10^5$.

4.3 Combined OVT and ACT

We consider combined therapy of OVT and ACT in this subsection. In Figure 7(a)-(b), $\beta = 0.6$, $k = 10^{-5}$, $m = -10^{-6}$, $s_1 = 10^5$ and $s_2 = 10^3$ with initial condition $(2 \times 10^7, 0, 0, 300)$ are fixed. The anti-viral killing rate γ is 0.9 in Figure 7(a) and 0.09 in Figure 7(b). We see that if γ is reduced, the ACT is more valuable and effective. The OVT needs not to be implemented for the whole treatment period and the tumor can be reduced further with oscillations under more frequent ACT. In Figure 7(c), $\beta = 0.9$, $k = 10^{-5}$, $m = -10^{-6}$, $\gamma = 0.09$, $s_1 = 10^4$ and $s_2 = 10^2$ with initial condition $(2 \times 10^7, 0, 0, 300)$. The virus is more transmissible but with a smaller dose of OVT. The OVT is applied for the whole treatment period in order to control the tumor.
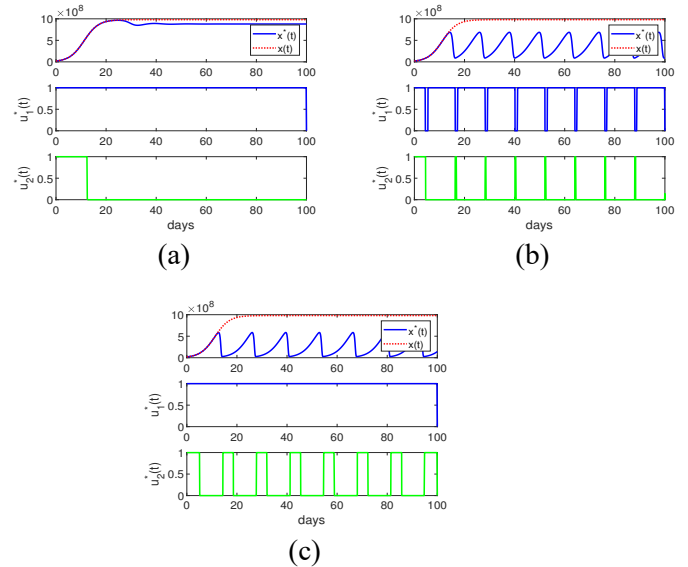

(a)

(b)

(c)

Figure 7: $k = 10^{-5}$, $m = -10^{-6}$ with initial condition $(2 \times 10^7, 0, 0, 300)$. Then $s_{2cri} = 3.3991 \times 10^7$. (a) $\beta = 0.6, \gamma = 0.9, s_1 = 10^5, s_2 = 10^3$. (b) $\beta = 0.6, \gamma = 0.09, s_1 = 10^5, s_2 = 10^3$. (c) $\beta = 0.9, \gamma = 0.09, s_1 = 10^4, s_2 = 10^2$.

In Figure 8, $\beta = 0.9, \gamma = 0.09, m = -10^{-6}, s_1 = 10^4, s_2 = 10^2$ and initial condition $(2 \times 10^7, 0, 0, 300)$ are fixed. We vary the anti-tumor killing rate k with $k = 8 \times 10^{-4}$, 7×10^{-4} and 6×10^{-4} in Figure 8(a), (b) and (c), respectively. Since the anti-vrial killing rate $\gamma = 0.09$ is small, ACT does not affect much of the OVT efficacy. The OVT has to be applied for the

whole treatment period when k is small. The therapy does not need to be employed for the whole treatment period when k is larger.
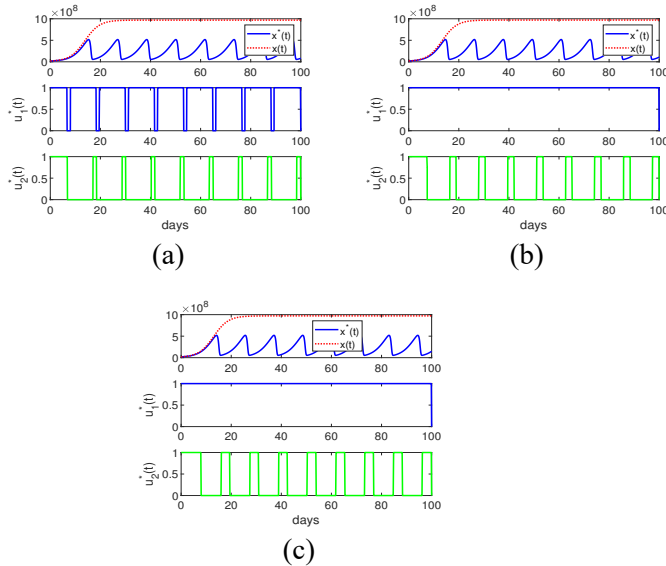

(a)

(b)

(c)

Figure 8: $\beta = 0.9$, $\gamma = 0.09$, $m = -10^{-6}$, $s_1 = 10^4$, $s_2 = 10^2$ with initial condition $(2 \times 10^7, 0, 0, 300)$ are fixed. (a) $k = 8 \times 10^{-4}$. (b) $k = 7 \times 10^{-4}$. (c) $k = 6 \times 10^{-4}$.

Comparing Figures 7 and 8, notice that when $\gamma = 0.9$ is large in Figure 7(a), the ACT is detrimental to the effectiveness of OVT and thus ACT is only applied initially and the tumor is not reduced significantly. When γ gets smaller with $\gamma = 0.09$ in Figure 7(b), the ACT and OVT work somewhat synergistically and the tumor can be controlled with oscillations. The tumor can be reduced further if $\beta = 0.9$ given in plot (c) of Figure 7.

Finally, $k = 10^{-5}$, $m = -10^{-6}$, $s_1 = 10^5$, $s_2 = 10^3$ with initial condition $(2 \times 10^7, 0, 0, 300)$ are fixed while varying β and γ in Figure 9. Comparing plots (a) and (b), as γ is increased, the ACT is detrimental to the effectiveness of OVT and thus the ACT is only applied in the beginning of the treatment period. As γ is increased further but with a larger infection rate β, the ACT can be applied intermittently as shown in plot (c).
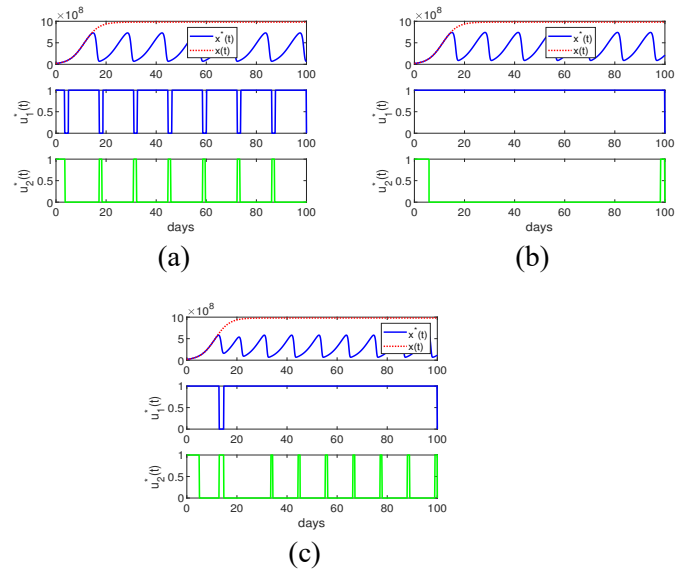

(a)

(b)

(c)

Figure 9: $k = 10^{-5}$, $m = -10^{-6}$, $s_1 = 10^5$, $s_2 = 10^3$ with initial condition $(2 \times 10^7, 0, 0, 300)$ are fixed for all the simulations. (a) $\beta = 0.5$, $\gamma = 0.06$. (b) $\beta = 0.5$, $\gamma = 0.07$. (c) $\beta = 0.8$, $\gamma = 0.1$.

5   Summary and Conclusion

In this study, we apply optimal control techniques to investigate effectiveness of the oncolytic viral therapy and adopted T cell transfer over a short time treatment period. Specifically, the model of no control is based on an earlier study given in [37] where a mathematical model of the tumor-immune system interactions with OVT was studied. The authors in [37] derived several sufficient conditions in terms of model parameters for which the susceptible tumor cells can be eradicated for all sizes. However, these results are based on the asymptotic dynamics of the tumor which may not be applicable in real life scenarios.

The goal of the control is to minimize the number of susceptible tumor cells along with the costs or the tolerances associated with the therapy. We do not minimize the number of infected tumor cells since these cells do not proliferate. As immune cells can kill viruses from the OVT, the two types of therapy do not provide synergistic effects. This is especially true when the viral killing rate γ is large. When the dosage s_2 of ACT is larger than the critical size derived in [37], the susceptible tumor cells can be eradicated by the first 20 days as shown in Figure 6. In general, the monotherapy of OVT is more effective if the viral infection rate β is larger while the viral killing rate γ is smaller even when the tumor microenviroment is very immunosuppressive. See Figures 1–3. If the initial tumor size is smaller, that is, $x(0) = 10^7$ instead of $x(0) = 2 \times 10^7$, the OVT needs not to be imple-

mented for the whole treatment period and the susceptible tumor exhibits dormant and elapse phenomenon shown in Figures 4 and 5. For the combined therapy of OVT and ACT, the ACT is not useful on controlling the tumor if anti-viral killing rate γ is large as shown in Figures 7–9. From these simulations, we conclude that sole OVT is more effective than the sole ACT if s_2 is below the critical value. However, if s_2 is above the threshold, then the susceptible tumor cells can be eradicated less than 100 days while the results obtained in [37] are with respect to the long term dynamics of the susceptible tumor cells.

References:

[1] Apolonio J, de Souza Gonçalves V, Santos ML, Luz M, Souza JV, Pinheiro SL, de Souza WR, Loureiro M, de Melo FF. Oncolytic virus therapy in cancer: A current review, *World J Virol.*, **210**(5), 2021, 229-255.

[2] Burden, T., Ernstberger, J., Fister, K., Optimal control applied to immunotherapy, *Dis. Cont. Dyn. Sys. Ser.* B, **4**, 2004,135-146.

[3] Choudhury B, Nasipuri B, Efficient virotherapy of cancer in the presence of immune response, *Int. J. Dynam. Control*, **2**, 2014, 314-325.

[4] Deer EL, et al., Phenotype and genotype of pancreatic cancer cell lines, *Pancreas*, **39**(4),2010, 425-435.

[5] de Matos AL, Lina S. Franco LS, McFadden G, Oncolytic viruses and the immune system: The dynamic duo, *Mol. Ther. Methods Clin. Dev.*, **17**,2020, 349-358.

[6] de Pillis L, Radunskaya A, Wiseman C, A validated mathematical model of cell-mediated immune response to tumor growth. *Cancer Res.*, **65**(17),2005,7950-7958.

[7] Dong H, Markovic SN, *The Basics of Cancer Immunotherapy*, Springer 2018.

[8] Eftimie R, et al., Interaction between the immune system and cancer: a brief review of non-spatial mathematical models, *Bull. Math. Biol.*, **73**, 2011, 2-32.

[9] Eftimie R, Eftimie G, Tumour-associated macrophages and oncolytic virotherapies: a mathematical investigation into a complex dynamics, *Lett. Biomath.* **5**, 2018, 6-35.

[10] Ferrucci P, Pala L, Conforti F, Emilia Cocorocchio E, Talimogene Laherparepvec (T-VEC): An intralesional cancer immunotherapy for advanced melanoma, *Cancers*, **13**, 2021, 1383. https://doi.org/10.3390/cancers13061383.

[11] Fleming, W., Rishel, R., *Deterministic and Stochastic Optimal Control*, Springer, New York, 1975.

[12] Fukuhara H, Ino Y, Todo T, Oncolytic virus therapy: A new era of cancer treatment at dawn. *Cancer Sci.*, **107**, 2016, 1373-1379.

[13] Garcia V, Bonhoeffer S, Fu F, Cancer-induced immunosuppression can enable effectiveness of immunotherapy through bistability generation: A mathematical and computational examination, *J. Theor. Biol.*, **492**, 2020, 110185.

[14] Gujar S, Pol JG, Kim Y, et al., Antitumor benefits of antiviral immunity: An underappreciated aspect of oncolytic virotherapies, *Trends Immunol.*, **39**, 2018, 209-221.

[15] Gun S, et al., Targeting immune cells for cancer therapy, *Redox Biol.*, doi: 10.1016/j.redox.2019.101174.

[16] Haddad D, Genetically engineered vaccinia viruses as agents for cancer, treatment, imaging, and transgene delivery, *Front. Oncol.*, **7**, 2017, 1-12.

[17] Hale DF, Vreeland TJ, Peoples GE, Arming the immune system through vaccination to prevent cancer recurrence, *Am. Soc. Clin. Oncol. Educ. Book.*, **35**, 2016, e159-e167.

[18] Hanada K, et al., An effective mouse model for adoptive cancer immunotherapy targeting neoantigens, *JCI Insight*, JCI Insight. 2019(10), e124405.

[19] Hanahan D, Weinberg RA, Hallmarks of cancer: the next generation, *Cell*, **144**(5), 2011, 646-674.

[20] Hu X, Jang R-J S, Optimal treatments in cancer immunotherapy involving CD4$^+$ T cells, *WSEAS Trans. Biol. Biomed.*, **15**, 2018, 48-67.

[21] Hu X, Ke G, Jang R-J S, Modeling pancreatic cancer dynamics with immunotherapy, *Bull. Math. Biol.*, **81**, 2019, 1885-1915.

[22] Jang R-J S, Wei H-C, On a mathematical model of tumor-immune system interactions with an oncolytic virus therapy, *Discrete Contin. Dyn. Syst. Ser. B*, **27**(6), 2022, 3261-3295.

[23] Kim KS, Kim S, Jung I, Hopf bifurcation analysis and optimal control of Treatment in a delayed oncolytic virus dynamics, *Math. Comput. Simul.*, **149**, 2018, 1-16.

[24] Koujima T, Tazawa H, Ieda T, et al., Oncolytic virus-mediated targeting of the ERK signaling pathway inhibits invasive propensity in human pancreatic cancer, *Mol. Ther. Oncolytics*, **17**, 2020, 107-117.

[25] Kuznetsov VA, Makalkin IA, Taylor MA, Perelson AS, Nonlinear dynamics of immunogenic tumors: parameter estimation and global bifurcation analysis, *Bull. Math. Biol.*, **56**(2), 1994, 295-321.

[26] Laird AK, Dynamics of tumor growth, *Br. J. Cancer*, **18**, 1964, 490-502.

[27] Lenhart, L., Workman, JT., *Optimal Control Applied to Biological Models*, Chapman & Hall: New York, 2007.

[28] Malinzi J, et al., Enhancement of chemotherapy using oncolytic virotherapy: Mathematical and optimal control analysis, *Math. Biosci. Eng.*, **15**, 2018, 1435-1463.

[29] Magen A, Nie J, Ciucci T, et al., Single-cell profiling defines transcriptomic signatures specific to tumor-reactive versus virus-responsive CD4$^+$ T cells, *Cell Reports*, **29**, 2019, 3019-3032.

[30] Mahasa KJ, Eladdadi A, de Pillis L, Ouifki R, Oncolytic potency and reduced virus tumorspecificity in oncolytic virotherapy. A mathematical modelling approach, *PLoS ONE*, **12**(9), 2017, 1-25.

[31] Marelli G, Howells A, Lemoine NR, Wang Y, Oncolytic viral therapy and the immune system: A double-edged sword against cancer, *Front. Immunol.*, **9**, 2018, 1-9.

[32] Okamoto K, Amarasekare P, Petty I, Modeling oncolytic virotherapy: Is complete tumor–tropism too much of a good thing? *J. Theor. Biol.*, **358**, 2014, 166-178.

[33] Rosenberg SA, et al., Adoptive cell transfer: a clinical path to effective cancer immunotherapy, *Nat Rev Cancer*, **4**(8), 2000, 10.1038/nrc2355.

[34] Storey KM, Lawler SE, Jackson TL, Modeling oncolytic viral therapy, immune checkpoint inhibition, and the complex dynamics of innate and adaptive immunity in glioblastoma treatment, *Front. Physiol.*, **11**, 2020, 1-18.

[35] Su Y, Jia C, Chen Y, Optimal Control Model of Tumor Treatment with Oncolytic Virus and MEK Inhibitor, *Biomed Res. Int.*, Volume 2016, 2016, 5621313.

[36] Vinay D et al., Immune evasion in cancer: Mechanistic basis and therapeutic strategies, *Semin. Cancer Biol.*, **35**, 2015, S185-S198.

[37] Vithanage R., Wei H-C, Jang S R-J., Bistability in a model of tumor-immune system interactions with an oncolytic viral therapy, *Math. Biosci. Eng.*, **19**(2), 2022, 1559-1587.

[38] Wodarz D, Viruses as antitumor weapons, *Cancer Res.* **61**, 2001, 3501-3507.

[39] Wodarz D, Komarova N, Towards predictive computational models of oncolytic virus therapy: Basis for experimental validation and model selection, *PLoS ONE*, **4**, 2009, e4271.

[40] Wu JT, Byrne HM, Kirn DH, Wein LM, Modeling and analysis of a virus that replicates selectively in tumor cells, *Bull. Math. Biol.*, **63**, 2001, 731-768.

Contribution of individual authors to the creation of a scientific article (ghostwriting policy)

Conceptualization: Sophia Jang, Rohana Vithanage;
Formal analysis: Rohana Vithanage, Sophia Jang;
Numerical Simulations: Rohana Vithanage, Sophia Jang;
Writing: Sophia Jang, Rohana Vithanage

Follow: www.wseas.org/multimedia/contributor-role-instruction.pdf

Creative Commons Attribution License 4.0 (Attribution 4.0 International , CC BY 4.0)